Development of a Similarity Analysis System with Various Techniques and Its Applications to LEU+ Fuel-Loaded Critical Assembly Designs Using McCARD

Min Ju Kim [a] and Ho Jin Park [a*]
[a] *Kyung Hee University, 1732, Deogyeong-daero, Giheung-gu, Yongin-si, 17104, Korea*

[*] *Corresponding author: parkhj@khu.ac.kr*

Keywords : Similarity Analysis, Critical Assembly Design, Criticality Experiment Benchmark, LEU+, i-SMR

1. Introduction

When designing new types of nuclear reactors, it is essential to verify the design methods and tools to ensure adequate safety margins. This validation process usually involves comparing code calculation results with experimental data, particularly criticality experiment benchmarks. Accordingly, selecting appropriate criticality experimental benchmarks that accurately represent the target system is crucial for quantifying the computational code uncertainties and biases.

Recently, innovative SMR (i-SMR) concepts employing LEU+ fuels (^{235}U enrichment 5 ~ 10 wt.%) have attracted increasing attention [1]. In a previous study, the LEU+ fuel-loaded i-SMR was adopted as the target system, and the computational code was validated through comparisons with selected criticality benchmark experiments conducted at the same enrichment level [2]. To apply quantitative criteria for benchmark selection, a follow-on study employed the deterministic sensitivity and uncertainty (S/U) based similarity coefficient, c_k, and evaluated similarity between the target system and criticality benchmarks [3]. However, the correspondence between the similarity coefficient and the similarity of the neutron energy spectrum was inconsistent. This observation indicates that reliance on the c_k for the multiplication factor alone may not fully capture the underlying neutronic representativity between systems, particularly when spectral characteristics differ.

Moreover, previous similarity analyses have primarily focused on covariance data for the dominant fuel nuclides, ^{235}U and ^{238}U. However, in i-SMR systems, many nuclides present in the moderator and structural materials may also contribute to system uncertainty. Therefore, the objectives of this study are (1) to quantify the impact of covariance nuclide selection on the S/U based similarity coefficient, (2) to evaluate and compare various neutron energy spectrum similarity measures, and (3) to preliminarily apply the developed similarity analysis system to the design of a critical assembly similar to a LEU+ fuel-loaded i-SMR system.

The S/U-based similarity analysis was performed using McCARD Monte Carlo code [4] with the SIMTEST utility [5], and the spectral similarity analysis was carried out using McCARD coupled with an in-house Python utility.

2. Similarity Analysis Generation

2.1 S/U-Based Similarity Coefficient

Some researchers quantified the degree of similarity between two systems [6-7]. The similarity coefficient, c_k, based on the sensitivity and uncertainty (S/U) method is defined as the Pearson correlation coefficient [8]. Here $cov\,[k_I, k_{II}]$ and $\sigma(k)$ represent the covariance and standard deviations of k_{eff} due to nuclear data uncertainties.

$$c_k = \frac{cov\,[k_I, k_{II}]}{\sigma(k_I) \cdot \sigma(k_{II})} \tag{1}$$

Using the 1st-order S/U propagation, Eq. (1) can be equivalently recast as Eq. (2).

$$c_k = \frac{S_I^T C S_{II}}{\sqrt{S_I^T C S_I}\sqrt{S_{II}^T C S_{II}}} \tag{2}$$

S_I and S_{II} are the sensitivity coefficient vectors of k_{eff} for system I and II, respectively, and S^T denotes the transpose of S. The matrix C denotes covariance data whose elements are $cov\,[x_{\alpha,g}^{i}, x_{\alpha',g'}^{i'}]$, obtained from an evaluated nuclear data library. The similarity coefficient c_k ranges from -1 to 1, and values close to 1 indicate a strong positive correlation between two systems.

$$S = \frac{\partial k}{\partial x_{\alpha,g}^{i}} \tag{3}$$

The sensitivity coefficient vector S contains sensitivities of the calculated k_{eff} with respect to the $x_{\alpha,g}^{i}$, α-type microscopic cross-section of isotope i for energy group g.

2.2 Neutron Energy Spectrum Similarity Measures

Compared to other fields, the quantitative analysis of neutron energy spectrum similarity has received relatively little attention in the fields of reactor physics and nuclear criticality safety. In order to complement the

similarity coefficient for multiplication factor, spectral similarity measures are introduced to directly compare the neutron energy spectra of two systems.

Before performing similarity calculation, neutron flux spectrum is normalized to remove the influence of absolute flux magnitude. In addition, the group-wise neutron flux is expressed on a lethargy basis by dividing the lethargy width of each group. The normalized neutron flux of energy group g of system I, denoted as $s_{g,I}$, is defined as

$$s_{g,I} = \frac{\phi_{g,I} / \Delta u_g}{\sum \left(\phi_{g,I} / \Delta u_g \right)} \tag{4}$$

where $\phi_{g,I}$ is the neutron flux in energy group g of system I, G is the total number of energy groups and Δu_g is the lethargy width of group g, defined as

$$\Delta u_g = ln\left(\frac{E_g}{E_{g-1}}\right) \tag{5}$$

Here, E_{g-1} and E_g are the upper and lower energy boundaries of group g, respectively. Therefore, $\phi_{g,I} / \Delta u_g$ represents the neutron flux per unit lethargy.

Regarding spectral similarity, the neutron energy spectrum similarity index, S, has been introduced to the MONK Coupling Similarity analysis code (MCS) [9]. In addition, various similarity measures widely used in data analysis have been adopted for spectral comparison, including the Pearson's product-moment correlation coefficient (PCC), the cosine metric, and Jensen-Shannon divergence (JSD) [10].

The index S based on neutron energy spectrum is defined as follows:

$$S = \sum_{g=1}^{G} \frac{s_{g,I} + s_{g,II}}{2} \frac{min(s_{g,I},\ s_{g,II})}{max(s_{g,I}, s_{g,II})} \tag{6}$$

The physical characteristic of the index S quantifies the degree of overlap between the group-normalized neutron flux distributions. Because it penalizes discrepancies in each energy group through the min/max ratio, it is sensitive to local spectral mismatches. Therefore, this index reflects not only the global spectral shape but also localized differences in specific energy regions [9].

The Pearson correlation coefficient (PCC) evaluates the linear correlation between two normalized neutron flux spectra after removing their mean values:

$$PCC(s_I, s_{II}) = \frac{\sum_{g=1}^{G}\left(s_{g,I} - \overline{s_I}\right)\left(s_{g,II} - \overline{s_{II}}\right)}{\sqrt{\sum_{g=1}^{G}\left(s_{g,I} - \overline{s_I}\right)^2}\sqrt{\sum_{g=1}^{G}\left(s_{g,II} - \overline{s_{II}}\right)^2}} \tag{7}$$

By centering each spectrum, PCC measures the similarity of group-wise deviations from the average flux level. Its value ranges from −1 to 1, where unity indicates perfectly correlated spectral fluctuations. Because the mean component is excluded, PCC reflects relative spectral variations rather than absolute distribution characteristics.

The cosine metric measures the angular similarity between two spectral vectors in energy-group space:

$$cos(s_I, s_{II}) = \frac{\sum_{g=1}^{G} s_{g,I}\ s_{g,II}}{\sqrt{\sum_{g=1}^{G} s_{g,I}^2}\sqrt{\sum_{g=1}^{G} s_{g,II}^2}} \tag{8}$$

It evaluates the directional similarity between two flux vectors in a high dimensional energy space. Since it depends only on the vector direction, cosine similarity is invariant to uniform scaling of the spectrum and primarily reflects global spectral shape similarity. However, it may become insensitive when two spectra share similar overall profiles, even if subtle local deviations exist.

Jensen-Shannon Divergence (JSD) is the metric representing distance between probability distributions. It provides a modification derived from the Kullback-Leibler (KL) divergence to satisfy symmetry property and is defined as [11]:

$$d_{JSD}(s_I, s_{II}) = \frac{1}{2} D_{KL}(s_I \parallel M) + \frac{1}{2} D_{KL}(s_{II} \parallel M)\,,$$

$$D_{KL}(s_I \parallel M) = \sum_g s_{g,I} \log_2 \frac{s_{g,I}}{m_g}\,,$$

$$m_g = \frac{1}{2}\left(s_{g,I} + s_{g,II}\right) \tag{9}$$

It quantifies how different two probability distributions are relative to their average distribution. Because the normalized neutron spectrum is treated as probability distribution, JSD measures the divergence in spectral shape. As a distance metric (d), JSD can be converted into a similarity (s) concept using $s = 1 - d$, when d is normalized in the range from 0 to 1 [10].

2.3 Similarity Analysis Code System

Calculations for similarity coefficients are performed using the McCARD and SIMTEST code system. Figure 1 shows the flowchart for similarity coefficient generation. The McCARD code has a MC perturbation technique for sensitivity coefficient generation due to the uncertainty of nuclear reaction cross-section. SIMTEST utility can generate c_k based on the deterministic S/U method, using the sensitivity coefficients from McCARD calculation and the cross-section covariance data from the evaluated nuclear data library.

For neutron energy spectrum similarity calculations, the energy-wise neutron flux is calculated using the McCARD tally function. Then similarities are calculated using a Python utility, and to ensure consistent scaling with the index S, PCC and JSD were post-processed into similarity measures within the range $[0, 1]$.

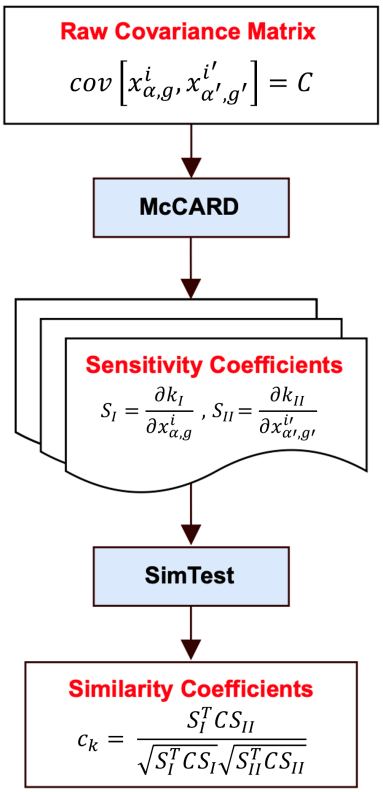

Fig 1. Flowchart to calculate similarity coefficients

3. Impact of Covariance Nuclide Selection on Similarity Coefficient

3.1 Covariance Set Configuration

To investigate the impact of nuclide variation on the S/U-based similarity coefficient, the ENDF/B-VII.1 covariance data processed in the LANL 30-group structure were used. The raw covariance data were grouped into three nuclide sets, as shown in Table I. Set 1 includes the major actinides contained in the fuel. Moderator nuclides were added in set 2, structural and absorber nuclides were added in set 3.

Table I. Nuclide sets included in the covariance matrix

set	Number of isotopes	Included nuclide isotopes
1	2	^{235}U, ^{238}U
2	4	^{235}U, ^{238}U, ^{1}H, ^{16}O
3	19	^{235}U, ^{238}U, ^{1}H, ^{16}O, ^{90}Zr, ^{91}Zr, ^{92}Zr, ^{93}Zr, ^{94}Zr, ^{95}Zr, ^{96}Zr, ^{152}Gd, ^{153}Gd, ^{154}Gd, ^{155}Gd, ^{156}Gd, ^{157}Gd, ^{158}Gd, ^{160}Gd

In constructing the raw covariance data, included reaction types were elastic scattering (MT=2), inelastic scattering (MT=4), capture (MT=102), $(n, 2n)$ reaction (MT=16), $(n, 3n)$ reaction (MT=17), particle-induced fission (MT=18), (n, p) reaction (MT=103), (n, α) reaction (MT=107) and $\bar{\nu}$ (MT=452).

For each set, similarity coefficients were recalculated for target-benchmark cases considered in the previous study [3]. Table II indicates calculation cases for each covariance set, and benchmark systems are from International Criticality Safety Benchmark Evaluation Project (ICSBEP) [12]. The first case was selected due to the reasonable value of c_k (0.876) and the high similarity in the neutron energy spectrum. The second case was selected because its c_k was high (0.922), despite the large difference in the neutron energy spectrum shown in Figure 2. Although LST020c1 employs the same 10 wt.% ^{235}U enrichment, its neutron energy spectrum is more thermalized than those of i-SMR 10 wt.% and LCT022c1 because it consists of a uranyl nitrate solution system with strong moderation.

Table II. Selected cases for similarity coefficient calculation

	Target System (I)	Benchmark System (II)
1	i-SMR 10 wt.%	LEU-COMP-THERM 22 c1 (10 wt.%)
2	i-SMR 2 wt.%	LEU-SOL-THERM 20 c1 (10 wt.%)

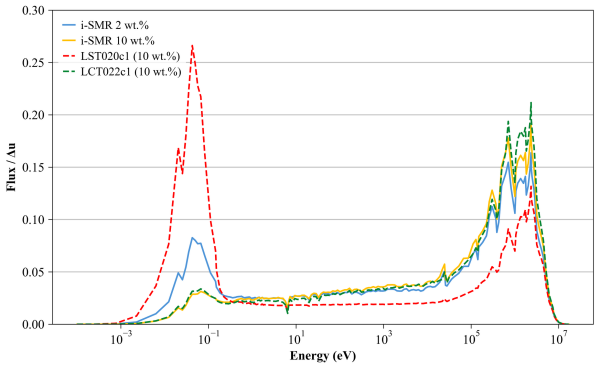

Fig 2. Neutron energy spectra of selected cases

3.2 Effect of Covariance Set Expansion on Similarity Coefficient

For the sensitivity coefficient generation, the McCARD eigenvalue calculation was performed using 200 inactive cycles and 800 active cycles, with 80,000 histories per cycle for covariance Set 1. For covariance Sets 2 and 3, 50 inactive cycles and 100 active cycles were used with 10,000 histories per cycle for computational efficiency.

Table III shows the calculation results between i-SMR 10 wt.% and LCT022c1 (10 wt.%), while Table IV shows the results between i-SMR 2 wt.% and LST020c1. As the number of nuclides included in the covariance increased, the nuclide-data-induced uncertainties $\sigma(k^I)$ and $\sigma(k^{II})$ increased, and the corresponding c_k values tended to decrease.

Table III. Results between i-SMR 10 wt.% and LCT022c1

set	c_k	$\sqrt{S_I^T C_{aa} S_I}$	$\sqrt{S_{II}^T C_{aa} S_{II}}$
1	**0.87555**	0.00803	0.00652
2	**0.82593**	0.00929	0.00834
3	**0.82147**	0.00934	0.00834

Table IV. Results between i-SMR 2 wt.% and LST020c1

set	c_k	$\sqrt{S_I^T C_{aa} S_I}$	$\sqrt{S_{II}^T C_{aa} S_{II}}$
1	**0.92185**	0.00715	0.00739
2	**0.82591**	0.00734	0.01092
3	**0.82098**	0.00739	0.01092

As shown in Tables III and IV, the $\sigma(k^I)$ values increased slightly with the covariance nuclide set expansion. However, $\sigma(k^{II})$ values exhibited a marked increase from covariance Set 1 to Set 2, while remaining unchanged from Set 2 to Set 3. Notably, the i-SMR 2 wt.% and LST020c1 pair showed a more pronounced reduction in c_k from Set 1 to Set 2 than the other case, motivating a nuclide-wise contribution of the total uncertainty using a modified SIMTEST utility.

Table V. Nuclide-wise $S^T CS/\Sigma S^T CS$ (%) of i-SMR 2 wt.%

	Set 1	Set 2	Set 3
^{235}U	77.289	73.705	72.827
^{238}U	22.711	16.842	16.641
^{1}H	-	9.396	9.284
^{16}O	-	0.058	0.057
Zr	-	-	1.172
Gd	-	-	0.020

Table VI. Nuclide-wise $S^T CS/\Sigma S^T CS$ (%) of LST020c1

	Set 1	Set 2	Set 3
^{235}U	98.653	46.424	46.424
^{238}U	1.347	0.593	0.593
^{1}H	-	52.167	52.167
^{16}O	-	0.816	0.816
Zr	-	-	0.000
Gd	-	-	0.000

Table V and VI present nuclide-wise contributions to nuclear data induced uncertainty in k_{eff} (normalized $S^T CS$). For the i-SMR 2 wt.% system, the uncertainty is still primarily driven by fuel actinides across all sets. Even after including other nuclides, ^{235}U and ^{238}U account for approximately 89%, while ^{1}H accounts for about 9% and Zr/Gd contributes minimally. In contrast, adding moderator nuclides (Set 2) to LST020c1 shifts the uncertainty distribution dramatically. LST020c1 system consists of a uranyl nitrate solution in a water tank, so in this case, ^{1}H becomes the dominant contributor at approximately 52%, while the contribution of ^{235}U decreases to approximately 46%. This pronounced change in the uncertainty explains the marked increase in $\sigma(k^{II})$ and the associated reduction in c_k from Set 1 to Set 2. Moreover, LST020c1 does not contain Zr/Gd, leading to no further change from Set 2 to Set 3.

This can be understood from Eq. (1) and (2). If the covariance matrix (Set 3) is partitioned into contributions from nuclides common to both systems ("com") and those present only in system I ("nc": Gd, Zr), the numerator becomes as Eq. (10) because $S_{nc}^{II} \approx 0$ for nuclides absent in system II.

$$cov_{com} = \underbrace{\sum_{n\in com} S_{n,I}^T C_n S_n^{II}}_{cov_{com}} + \underbrace{\sum_{n\in nc} S_{n,I}^T C_n S_n^{II}}_{=0} \quad (10)$$

For the denominator, $\sigma^2\left(k_{iSMR(I)}\right)$ and $\sigma^2\left(k_{LST020(II)}\right)$ can be expressed like Eq. (11) and (12) for each.

$$\sigma^2\left(k_{iSMR(I)}\right) = \underbrace{\sum_{n\in com} S_{n,I}^T C_n S_n^{II}}_{sd1_{com}^2} + \underbrace{\sum_{n\in nc} S_{n,I}^T C_n S_n^{II}}_{sd1_{nc}^2>0} \quad (11)$$

$$\sigma^2\left(k_{LST(II)}\right) = \underbrace{\sum_{n\in com} S_{n,I}^T C_n S_n^{II}}_{sd2_{com}^2} + \underbrace{\sum_{n\in nc} S_{n,I}^T C_n S_n^{II}}_{=0} \quad (12)$$

Therefore, when Set 3 covariance is applied, the similarity coefficient formula becomes the same as Eq. (13), although the resulting value decreases compared to that for Set 2. Inclusion of non-common nuclides in the covariance matrix introduces additional variance terms in the denominator of the similarity coefficient, while the cross-covariance contribution in the numerator remains unchanged. Consequently, the resulting value decreases despite no physical increase in shared sensitivity structure.

$$c_k = \frac{cov_{com}}{\sqrt{\sigma_{I,com}^2 + \boldsymbol{\sigma_{I,nc}^2}}\sqrt{\sigma_{II,com}^2}} \quad (13)$$

Accordingly, when using c_k as a representativity index between a target system and criticality experiment benchmarks, it is advisable to calculate c_k using nuclides present in both systems.

4. Similarity Test Results

4.1 Similarity Coefficient Recalculation with Expanded Covariance Set

In our previous study, c_k was evaluated using a covariance set 1 (^{235}U, ^{238}U) [3]. However, the results in Section 3.2 indicated that moderator nuclides can dominate the uncertainty in criticality experiment benchmarks, implying that an actinide-only covariance

set may not be sufficient for representativity assessment. Therefore, the c_k values were recalculated using the second covariance set (^{235}U, ^{238}U, ^{1}H, ^{16}O).

Table VII. c_k results using ^{235}U, ^{238}U covariance

	2 wt.%	4 wt.%	6 wt.%	8 wt.%	10 wt.%	LST020c1	LMT007c2	LCT022c1	LCT085c1
i-SMR 2wt.%	1.00	≈ 1.00	1.00	0.99	0.99	0.92	0.78	0.84	0.82
i-SMR 4wt.%	≈ 1.00	1.00	≈ 1.00	≈ 1.00	≈ 1.00	0.91	0.80	0.89	0.85
i-SMR 6wt.%	1.00	≈ 1.00	1.00	≈ 1.00	≈ 1.00	0.87	0.79	0.90	0.85
i-SMR 8wt.%	0.99	≈ 1.00	≈ 1.00	1.00	≈ 1.00	0.83	0.77	0.89	0.83
i-SMR 10wt.%	0.99	≈ 1.00	≈ 1.00	≈ 1.00	1.00	0.78	0.74	0.88	0.81
LST020c1 (10 wt.%)	0.92	0.91	0.87	0.83	0.78	1.00	0.75	0.72	0.88
LMT007c2 (4.95 wt.%)	0.78	0.80	0.79	0.77	0.74	0.75	1.00	≈ 1.00	≈ 1.00
LCT022c1 (10 wt.%)	0.84	0.89	0.90	0.89	0.88	0.72	≈ 1.00	1.00	0.96
LCT085c13 (6.5 wt.%)	0.82	0.85	0.85	0.83	0.81	0.88	≈ 1.00	0.96	1.00

Table VIII. c_k results using ^{235}U, ^{238}U, ^{1}H, ^{16}O covariance

	2 wt.%	4 wt.%	6 wt.%	8 wt.%	10 wt.%	LST020c1	LMT007c2	LCT022c1	LCT085c13
i-SMR 2wt.%	1.00	0.99	0.97	0.95	0.94	0.83	0.73	0.78	0.76
i-SMR 4wt.%	0.99	1.00	1.00	0.99	0.98	0.80	0.73	0.80	0.77
i-SMR 6wt.%	0.97	1.00	1.00	1.00	0.99	0.78	0.73	0.82	0.78
i-SMR 8wt.%	0.95	0.99	1.00	1.00	1.00	0.76	0.73	0.82	0.77
i-SMR 10wt.%	0.94	0.98	0.99	1.00	1.00	0.74	0.72	0.83	0.77
LST020c1 (10 wt.%)	0.83	0.80	0.78	0.76	0.74	1.00	0.81	0.79	0.82
LMT007c2 (4.95 wt.%)	0.73	0.73	0.73	0.73	0.72	0.81	1.00	0.98	1.00
LCT022c1 (10 wt.%)	0.78	0.80	0.82	0.82	0.83	0.79	0.98	1.00	0.99
LCT085c13 (6.5 wt.%)	0.76	0.77	0.78	0.77	0.77	0.82	1.00	0.99	1.00

As shown in Tables VII and VIII, including the moderator nuclides in the covariance set changes the similarity coefficient values. For most i-SMR and benchmark pairs, c_k is lower than in the actinide-only case, because the benchmark uncertainty includes a strong moderator component that is not captured by Set 1. However, for some benchmark-benchmark pairs, c_k increased when moderator covariance was included; for example, the c_k between LCT022c1 and LCT085c13 increased from 0.957 to 0.991.

Additionally, Table VIII shows that the c_k between i-SMR 10 wt.% and LCT022c1, which had similar neutron energy spectra in Figure 2, is 0.826. Therefore, judging the similarity between the two systems based solely on the similarity coefficient for the multiplication factor remains difficult.

4.2 Neutron Energy Spectrum Similarity Tests

Based on the methods introduced in Section 2.2, spectrum similarity between several systems was compared using index S, PCC, cosine metric, and JSD. Table IX indicates selected cases for the similarity tests.

Table IX. Selected cases for spectrum similarity calculation

case	Target System (I)	Benchmark System (II)
1	i-SMR 10 wt.%	LEU-SOL-THERM 20 c1 (10 wt.%)
2	i-SMR 2 wt.%	LEU-SOL-THERM 20 c1 (10 wt.%)
3	i-SMR 4 wt.%	LEU-MEU-THERM 07 c2 (4.05 wt.%)
4	i-SMR 10 wt.%	LEU-COMP-THERM 22 c1 (10 wt.%)
5	i-SMR 6 wt.%	LEU-COMP-THERM 85 c13 (6.5 wt.%)

To generate neutron flux for 190 groups, all McCARD eigenvalue calculations were conducted under the condition of 500 inactive and 1000 active cycles, with 200,000 histories per cycle.

Table X summarizes the spectrum similarity results obtained using index S, Pearson correlation coefficient (PCC), cosine metric, and Jensen-Shannon divergence (JSD). To evaluate the effectiveness of each measure, the numerical results are compared with the visual spectral differences shown in Figures 3 and 4.

A meaningful spectral similarity index should exhibit sufficient dynamic range to discriminate between moderately similar and highly similar spectra. In Cases 1-3, noticeable spectral differences are observed, particularly in the thermal and epithermal energy regions. For these cases, Index S produces relatively lower similarity values, consistent with the visible discrepancies in the spectra.

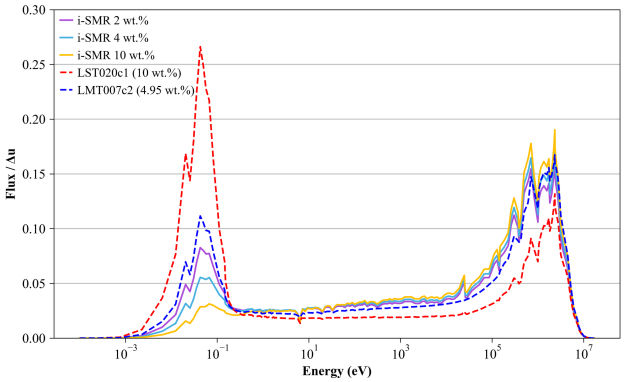

Fig 3. Neutron energy spectra of case 1, 2 and 3

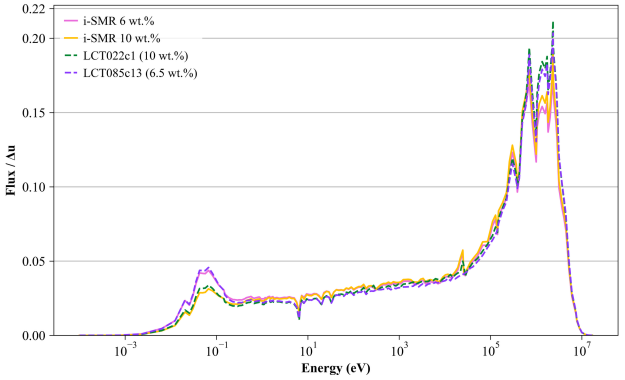

Fig 4. Neutron energy spectra of case 4 and 5

Table X. Spectrum Similarity Test Results using 4 methods

Case	c_k	**Index S**	**PCC**	**Cosine**	**JSD**
1	0.740	0.630	0.710	0.693	0.891
2	0.826	0.692	0.819	0.809	0.943
3	0.730	0.641	0.749	0.731	0.916
4	0.826	0.918	0.997	0.996	0.998
5	0.775	0.906	0.997	0.995	0.998

In contrast, for Cases 4 and 5, the spectra exhibit a significant degree of visual similarity. While PCC,

cosine, and JSD effectively estimate high similarity values close to unity, these measures tend to saturate near 1.0, thereby limiting their ability to discriminate subtle but systematic spectral differences. This behavior arises because these measures primarily evaluate global spectral shape similarity and are less sensitive to localized group-wise mismatches. Conversely, Index S provides a broader spectrum of similarity values (0.630-0.918 across all cases) and maintains distinguishability between moderately similar and highly similar systems. Given that Index S incorporates energy-group-wise min/max ratios, it is evident that it penalizes local spectral deviations more strongly than the other measures. Therefore, index S provides enhanced resolution in distinguishing group-wise flux mismatches.

Based on these observations, index S was selected as the primary neutron energy spectrum similarity measure in this study.

5. Preliminary Application of Similarity Framework to Critical Assembly Design

5.1 Baseline Critical Assembly Configuration

A preliminary critical assembly was developed to investigate the applicability of the enhanced similarity analysis framework for representativity-oriented experimental design. This assembly consists of a 3x3 lattice of A1-type fuel assemblies with 8 wt.% and 10 wt.% ^{235}U enrichment, respectively. Criticality was achieved by adjusting the moderator height, the primary reactivity control parameter in the proposed assembly. The reference configuration of the critical assembly was constructed by adapting the geometric features and material compositions of the LEU+ fuel-loaded i-SMR core. Based on this baseline configuration, a series of parametric cases were generated by varying the assembly gap while maintaining an identical fuel composition, axial configuration, and reflector structure. Modifying only the assembly pitch changed the moderation condition of the critical assembly without introducing additional geometric details. For each configuration, the moderator height was adjusted to achieve criticality.

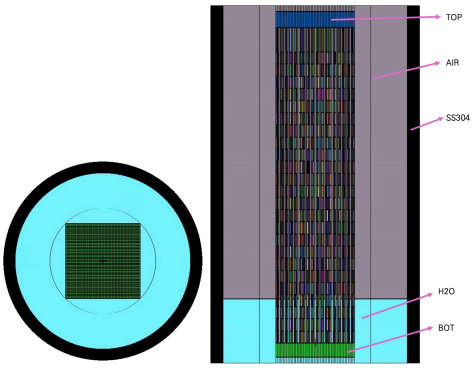

Fig 5. Cross-section of critical assembly

5.2 Similarity Tests for Designed Critical Assemblies

For each configuration with a modified assembly gap, similarity tests were performed against the i-SMR reference system using both the S/U-based similarity coefficient for the multiplication factor and the neutron energy spectrum similarity index introduced in Section 4. The assembly gap was varied from 0.005 cm to 3.0 cm, where 0.04 cm corresponds to the reference i-SMR configuration.

Figure 6 presents the critical moderator height required to achieve criticality as a function of assembly gap. As the assembly gap increases, neutron leakage and moderation effects change simultaneously, leading to a non-linear variation in the required moderator height. For very small gaps ($\leq$ 0.04 cm), the fuel lattice becomes more compact, reducing neutron leakage and increasing neutron utilization within the fuel region. Consequently, a relatively larger moderator height is required to balance reactivity. As the gap increases toward 1.0 cm, enhanced neutron moderation within the assembly gap region softens the spectrum and reduces the moderator height. Further increases beyond 2.0 cm increase neutron leakage, again requiring a higher moderator height.

Figures 7 and 8 show the variation of c_k and S with assembly gap for the 8 wt.% and 10 wt.% cases. Although the overall trends are similar, the 10 wt.% case exhibits slightly lower spectral similarity values, indicating that the enrichment level also influences the moderation-leakage balance and spectral behavior.

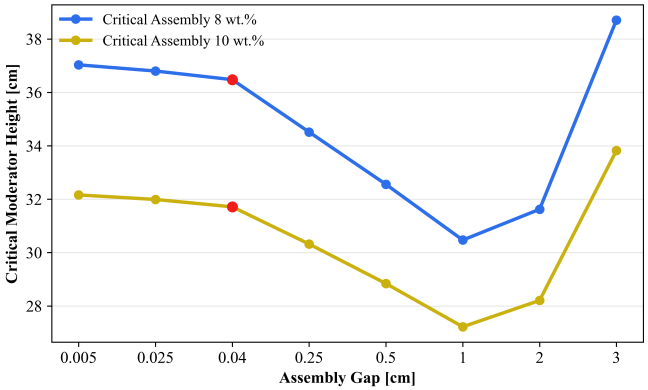

Fig 6. Critical moderator height according to assembly gap

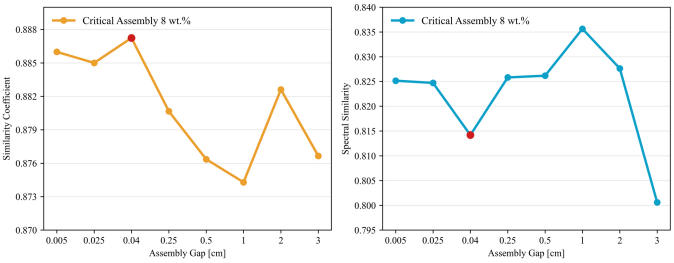

Fig 7. c_k and S according to assembly gap in 8 wt.% CA

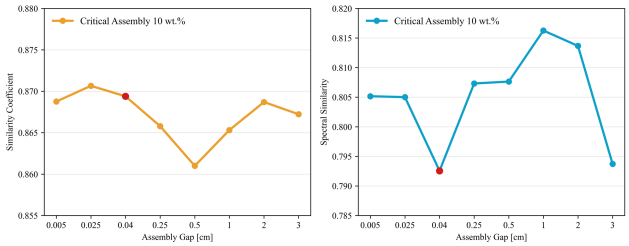

Fig 8. c_k and S according to assembly gap in 10 wt.% CA

However, the assembly gap giving the highest c_k is not the same as that giving the highest spectral similarity. For the 8 wt.% case, c_k is highest near the reference gap of the i-SMR system, whereas for the 10 wt.% case the maximum c_k is obtained at a different gap. In contrast, S is not highest at the reference gap in either case and tends to have higher values at moderate gaps. This indicates that agreement in the similarity coefficient for the multiplication factor does not necessarily guarantee agreement in neutron energy spectrum shape.

These results suggest that the S/U-based similarity coefficient and the spectral similarity should be considered together in the preliminary design of a representative critical assembly. While c_k reflects the similarity in multiplication-factor response to nuclear data uncertainty, the spectral similarity index S indicates how closely the neutron energy spectrum of a candidate design matches that of the target system. Therefore, the developed similarity analysis framework is useful for comparing candidate design options from different neutronic viewpoints during the preliminary design stage.

6. Conclusions

This study investigated the applicability of the developed similarity analysis system to the design of a critical assembly representative of a LEU+ fuel-loaded i-SMR system. Motivated by the previously observed inconsistencies between the deterministic sensitivity and uncertainty (S/U) based similarity coefficients for the multiplication factor and the neutron energy spectrum similarity, we systematically examined the roles of covariance nuclide selection and spectral similarity measures in representativity assessment.

First, the impact of covariance nuclide expansion on the similarity coefficient was quantified. The nuclide-wise uncertainty analysis demonstrated that moderator nuclides can dominate the uncertainty structure of the criticality experiment benchmark systems. Consequently, restricting the covariance set to fuel actinides may lead to distorted representativity evaluation. Based on this observation, it is recommended that the similarity coefficient be calculated using nuclides common to both the target and benchmark systems to avoid artificial degradation caused by non-common isotopes.

Second, neutron energy spectrum similarity was quantitatively evaluated using various candidate measures, including PCC, cosine similarity, JSD, and the adopted spectral similarity index S. While PCC, cosine, and JSD tended to approach unity for highly similar spectra - thereby limiting discrimination capability – the selected spectral similarity index S exhibited a wider dynamic range and better reflected visually observed spectral differences. Accordingly, the spectral similarity index S was adopted as the primary measure for spectral comparison in this study.

Finally, a preliminary critical assembly design study was conducted to explore the applicability of the developed similarity analysis system. Parametric variation of assembly gap revealed that the similarity coefficient for the multiplication factor and the spectral similarity index S respond differently to changes in moderation-leakage balance. The configuration showing the highest c_k did not always coincide with that giving the highest spectral similarity. These results indicate that the two measures characterize different but complementary physical aspects of reactor behavior.

The present study demonstrates that integrating the similarity coefficient for the multiplication factor with explicit spectral similarity assessment enables a more physically consistent representativity evaluation framework for LEU+ systems. Although the present analysis is limited to preliminary assembly configurations, the developed framework provides a practical basis for comparing candidate critical assembly designs from multiple neutronic viewpoints and supports preliminary critical assembly design for LEU+ fuel-loaded i-SMR systems.

ACKNOWLEDGEMENT

This work was supported by the National Research Foundation of Korea (NRF) grant funded by the Korea government (Ministry of Science and ICT) (No. RS-2024-00422848)

REFERENCES

[1] H. J. Jeong et al, Development of a Soluble Boron-Free SMR Core Using LEU+ Fuel with UO2-Gd2O3(Mo) Burnable Absorbers, The 34th Nuclear Energy for New Europe - NENE2025 conference, Bled, Slovenia, 8~11 September, 2025.
[2] M. J. Kim and H. J. Park, Validation of DeCART2D Criticality Calculations for LEU+ loaded SMR Systems, Transactions of the Korean Nuclear Society Autumn Meeting, Oct 24-25, 2024.
[3] M. J. Kim and H. J. Park, Criticality Experiment Benchmark Selection and New Critical Assembly Design Based on Similarity Analyses for LEU+ i-SMR System, Transactions of the Korean Nuclear Society Autumn Meeting, Oct 30-31, 2025.
[4] H. J. Shim et al., McCARD: Monte Carlo Code for Advanced Reactor Design and Analysis, Nuclear Engineering and Technology, Vol.44, p 161-176, 2012.
[5] H. J. Park and J. W. Park, Similarity Coefficient Generation Using Adjoint-Based Sensitivity and Uncertainty Method and Stochastic Sampling Method, Energies, 17, 827, 2024.

[6] B. L. Broadhead et al. Sensitivity- and Uncertainty-Based Criticality Safety Validation Techniques, Nuclear Science and Engineering, Vol 146, pp. 340-366, 2004.
[7] C. M. Perfetti and B. T. Rearden, Estimating Code Biases for Criticality Safety Applications with Few Relevant Benchmarks, Nuclear Science and Engineering, Vol 193, pp. 1090-1128, 2019.
[8] K. Pearson, Notes on Regression and Inheritance in the Case of Two Parents, Proc. R. Soc. London, Vol 58, pp. 240, 1895.
[9] Ning et al, Application of similarity analysis method in zero-power experimental validation, International Conference on Nuclear Data for Science and Technology, Sep 30, 2020.
[10] Yuta et al, Automated estimation of materials parameter from X-ray absorption and electron energy-loss spectra with similarity measures, Computational Materials, 2019.
[11] Deza, M. M. & Deza, E., Encyclopedia of Distances, Springer, 2016.
[12] International Handbook of Evaluated Criticality Safety Benchmark Experiments, OECD Nuclear Energy Agency report NEA/NSC/COD(95)03, 1998.